



Final Draft
of the original manuscript:

Zerbst, U.; Schoedel, M.; Beier, H.T.:

**Parameters affecting the damage tolerance behaviour of
railway axles**

In: Engineering Fracture Mechanics (2010) Elsevier

DOI: 10.1016/j.engfracmech.2010.03.013

PARAMETERS AFFECTING THE DAMAGE TOLERANCE BEHAVIOUR OF RAILWAY AXLES

Zerbst, U.^a, Schödel M. and ^b,Beier, H.Th.^c

^a GKSS Research Centre, Institute for Materials Research, Materials Mechanics,
D-21502 Geesthacht, Germany

^b formerly GKSS Research Centre, Institute for Materials Research, Materials Mechanics,
D-21502 Geesthacht, Germany

^c Technical University Darmstadt, IFSW, D-64287 Darmstadt, Germany

ABSTRACT

The paper provides a discussion on damage tolerance options applied to railway axles and factors influencing the residual lifetime as well as the required inspection interval. These comprise material properties such as the scatter of the da/dN- ΔK curve, the fatigue crack propagation threshold ΔK_{th} and the toughness of the material. Parameters affecting axle loading such as the press fit, rotating bending, load history and mixed crack opening modes are discussed. Finally the influence of the initial crack geometry on residual lifetime is simulated.

Key words. Railway axles, Damage tolerance, Fatigue Crack propagation

1. INTRODUCTION

One of the key events, and perhaps the most important one, which initiated the worldwide research in strength and failure of engineering components was a major accident caused by a broken railway axle. When one of the axles of a locomotive broke on the line between Paris and Versailles on 8 May 1842 a large number of passengers – estimates range between 60 and 100 or even more [1] –died in the fire spilt from the engine to the carriages. It was the first railway accident in which major loss of life occurred and it sent out shock waves round the globe although axle failures were anything but unusual in the 19th century. Still in the ten years between 1881 and 1891 “an average of 178 iron and 72 steel driving axles failed each year” in Britain, “with an average distance of failure of the order of 340 000 km” [1].

As a response to this problem the fatigue strength (S-N curve) concepts which still form the basis for the design of cyclically loaded components were developed by August Wöhler (1819-1914) and others. During the 20th century the number of failures of railway axles was reduced to about 5% [2] due to improved steels and assessment concepts. Yet a small number of failures still occur and the consequences still might be severe because a broken axle usually results in a derailment. Therefore and because of new challenges of modern railway systems such as high speed traffic and heavy transportation the further development of appropriate measures for avoiding axle fracture is still on the agenda. The investigations have to comprise both, reliable fatigue strength and damage tolerance concepts. Whilst the fatigue strength concepts have to guarantee that no fracture will occur during the axle’s projected lifetime the aim of the damage tolerance concept is to reliably detect a potential fatigue crack until it extends to its critical dimension.

The present paper deals with questions of damage tolerance analysis of railway axles. It provides a systematic investigation on factors influencing the residual lifetime and inspection interval of axles and draws conclusions for practical application.

2. DAMAGE TOLERANCE OF RAILWAY AXLES

2.1 Damage tolerance options

One of the problems fatigue strength concepts for axles are confronted with is the very high number of loading cycles an axle experiences during its life. In [1] a number of 2×10^8 cycles/year is given for the British railway system which is realistic for other railroad networks as well. With a service life of an axle expected to exceed 30 years this figure refers to a total of more than 6×10^9 cycles. For comparison: the common endurance limit for steel components is defined for 10^6 cycles. A number of 6×10^9 cycles certainly refers to what is designated as „giga-cycle fatigue“. It is well recognized today (see, e.g., the papers in [3]) that final fracture can occur even at loading amplitudes well below the common endurance limit after such a large number of loading cycles.

The giga-cycle fatigue phenomenon is one of the reasons why damage tolerance considerations are needed in complementation to the fatigue strength concepts for railway axles. The damage tolerance approach assumes the existence of fatigue cracks which potentially become unsafe during the projected lifetime. In order to avoid failure of the component regular non-destructive inspections (NDI) are carried out. In that context, damage tolerance analyses provide information either on the required inspection interval or on the minimum crack size which has to be detected for an existing inspection interval. These two options shall be briefly outlined later in this section.

There are typical sites where fatigue cracks initiate at an axle (Figure 1). Cracks (1) and (3) are press fit cracks underneath the wheel (1) and the gear (3). Press fit cracks can also occur at the disc brake seats. Crack (2) is initiated at the geometrical transition (T transition) next to the wheel seat. While the reason for initiating press fit cracks is fretting between the press fitted parts, crack initiation at the geometrical transition is promoted by the stress concentration due to the notch. Besides crack locations (1) to (3) cracks may also be initiated, e.g. at corrosion pits, at the shaft away from the press fit and stress concentration regions particularly in freight wagons.

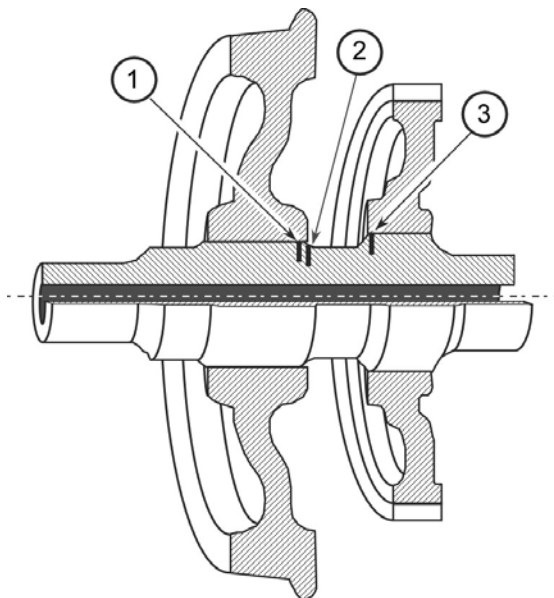


Figure 1: Typical fatigue crack locations in railway axles. (1) and (3) press fit cracks underneath the wheel and gear; (2) crack at geometrical transition (T transition).

Since the maximum bending stress occurs at the axle surface the surface finish is of major importance for crack initiation. Sometimes but rather seldom ballast impact causes local

notches which subsequently act as crack starters [4]. Analysing failure statistics the authors in [5] report on corrosion pits playing a major role as fatigue crack initiation sites. In order to avoid this coatings are applied to the axles. However, if a coating is locally damaged corrosion can occur as a much more severe localised problem. In [6] the authors have demonstrated that even a mildly corrosive substance such as rainwater can be detrimental in terms of fatigue crack propagation in axle material. Note that corrosion pits may also reduce the endurance limit of the axles by shortening the time needed for crack nucleation and early crack propagation [6]. Note that the fatigue strength is not a material and/or component property established once for all but can reduce during the lifetime of a component.

Crack nucleation and early crack propagation are not an issue of a damage tolerance analysis such as that described in this paper. Instead, the presence of a crack the size of which refers to the limits of non-destructive inspection is postulated. What matters is not the smallest crack which can be found under laboratory conditions but the largest crack that could escape detection under in-service conditions. For the present investigations the typical initial crack in railway axles was assumed to be semi-circular with a depth of 2 mm (see also [7]) although the authors in [1] assume a 5 mm deep crack as the smallest crack detectable by ultrasonic methods. Note that the specification of the initial crack size corresponds with a certain probability of detection (POD) of the crack by the non-destructive inspection technique applied. Following the first paper about POD of railway axles in 2001 [5] there has been an intense ongoing discussion on this topic (see, e.g. [8]). Two papers of the present issue [9,10] provide new POD data along with the data in [5] (Figure 2).

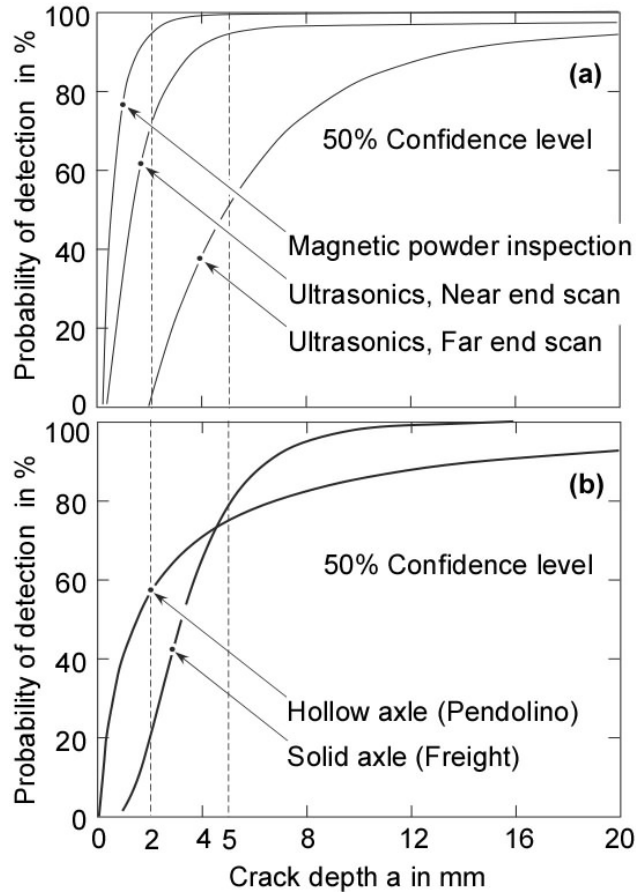


Figure 2: Probability of detection (POD) of cracks as a function of crack depth. (a) Data obtained by magnetic particle inspection and ultrasonic techniques (according to [5]; 50% confidence level; solid axle); (b) Comparison between ultrasonic near end scan data for solid axles and ultrasonic data obtained from the bore of hollow axles (according to [9]; 50% confidence level).

No detailed discussion on the determination of the POD will be given here since this is provided in [9] and [10]. Note that the probability of detection vs. crack depth characteristics strongly depends on the non-destructive inspection technique applied. The best results are obtained by magnetic particle inspection (Figure 2a) the application of which, however, requires open access to the axle surface, i.e. the wheels have to be dismounted from their wheel seats. On the other hand, since smaller defects can be found with high probability relatively large inspection intervals are possible which might permit the combination of the

inspections with regular wheelset overhauls this way saving costs for the operator [5]. For the relationship between the POD and the inspection interval see also the discussion in [11].

With respect to ultrasonic testing it has to be distinguished between near end/high angle scans performed from the axle surface and far end scans performed from one end of the axle. As can be seen from Figure 2a the far end scan method does not yield acceptable results and cannot be recommended for routine inspection [11]. In contrast to the magnetic powder method ultrasonic techniques do not require the removal of the wheels and bearings during testing. In hollow axles ultrasonic testing is performed from the bore which is advantageous with respect to accessibility. Figure 2b shows a comparison between POD data (50% confidence level) for a solid and a hollow axle according to [9]. It can be seen that the inspection from the bore (hollow axle) was superior to the near end scan inspection from the surface (solid axle) for smaller crack depths up to about 4 mm but it was inferior for larger cracks. However, care should be exercised with respect to any generalisation of this information because the data base of Figure 2b was rather limited.

Note that none of the curves in Figure 2 can be generalised because they belong to specific test setups. Modifications of the method, e.g., the application of a phase array technique (e.g., [12]) can improve the POD. Furthermore a key issue for improving the detection probability is to suppress the subjective aspect of testing, i.e., the skill of the operator and his power of concentration under varying conditions. In other words: What is needed is mechanisation and automation instead of manual testing [13].

There exist two basic options of a damage tolerance analysis the input parameters and basic steps of which are identical (Figure 3). The input information comprises the component geometry and dimension, the site of the fatigue crack and (usually) its potential plane of propagation, the size and shape of the initial crack, a_0 and $2c_0$, the loading of the component

which preferably should be known from dynamic simulation and test runs and material properties such as its stress-strain curve, its fracture toughness or statistical fracture toughness distribution and, most important, its fatigue crack propagation characteristics, i.e. its da/dN - ΔK curve. As the result of the analysis the crack depth is determined as a function of the time or number of loading cycles. Failure is defined by the fracture event or other criteria such as the wall breakthrough of the crack in a hollow axle (unless fracture occurs earlier).

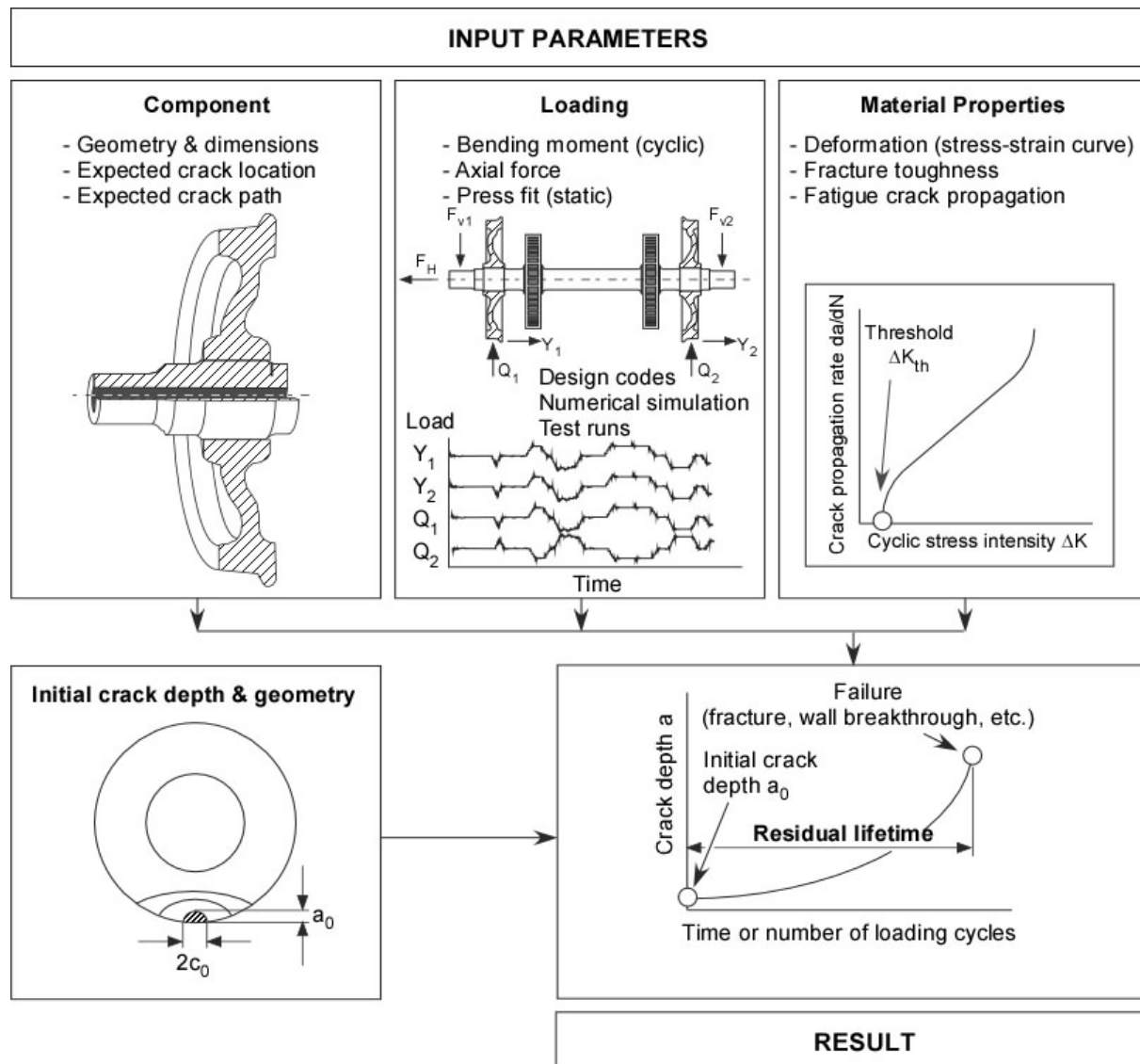


Figure 3: Input information and basic steps of a damage tolerance analysis of a railway axle.

What makes the difference between both assessment options is the target information (Figure 4):

Option A: Starting from the number of loading cycles at failure one inspection interval is subtracted such as illustrated in the figure. This way a crack depth a_d is determined which has to be found in an inspection. If it were missed the consequence would be failure at or immediately before the next inspection. Of course, even larger cracks will not be detected with certainty (see Figure 2). The probability of detecting a_d can simply be determined from Figure 2. It can be increased by reducing the inspection interval. In that case the crack to be found is larger and refers to a higher POD in Figure 2. Note that the crack depth a_d to be detected has to be larger than the chosen initial crack depth.

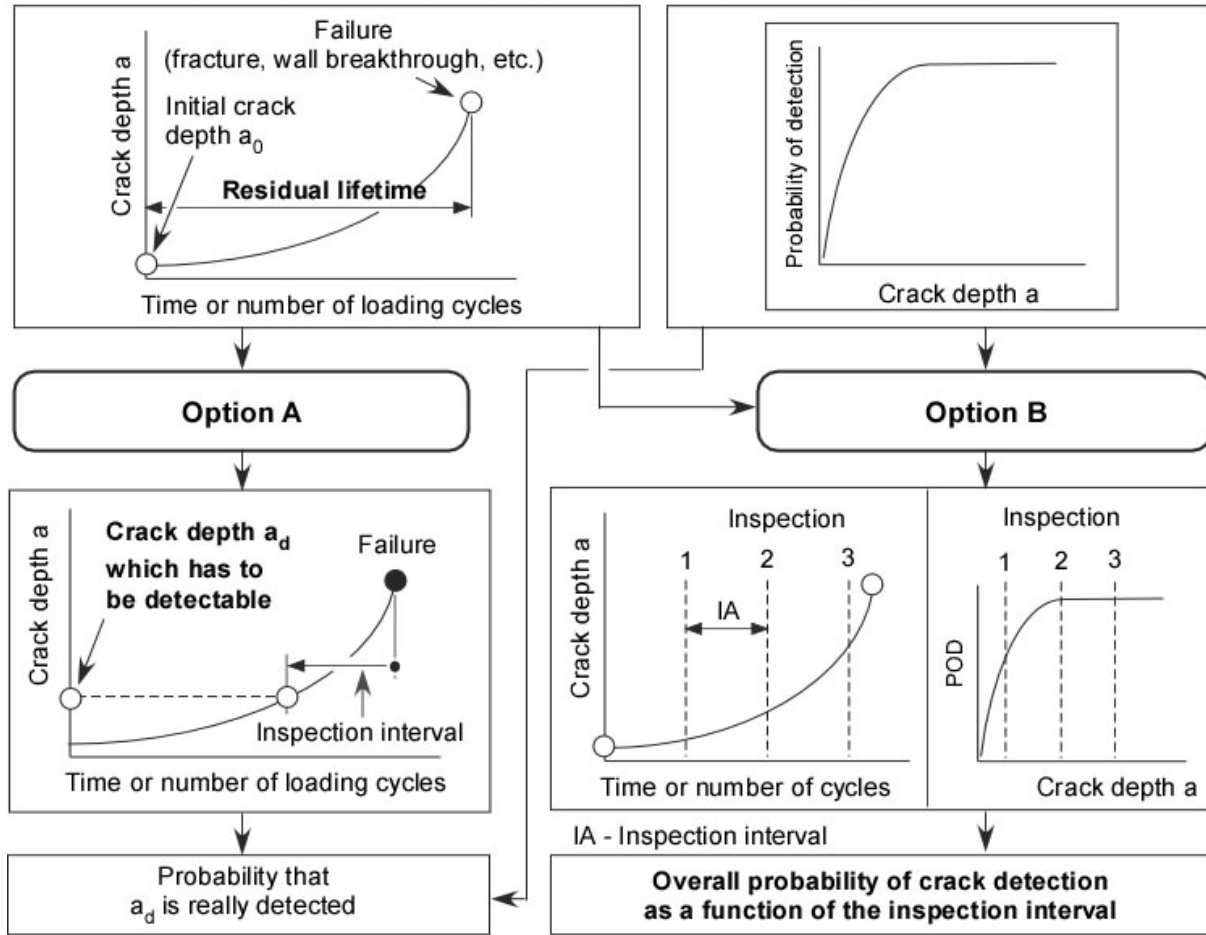
Option B: This option is based on the residual lifetime within which a number of inspections will be carried out depending on the inspection interval. Because the crack is extending the probability of detection is increased from inspection to inspection according to Figure 2. The overall probability of detection (POD) can easily be determined as the complement to the product of the non-detection probabilities (POND) of the i inspections carried out:

$$\text{POD}_{\text{overall}} = 1 - \left[\prod_i \text{POND}_i \right]. \quad (1)$$

Note that the result will be affected by the initial crack size chosen for the analysis.



From crack propagation analysis (Figure 3) NDI probability of detection POD (Fig. 2)



Improvement by smaller detectable initial crack sizes and/or by reducing the inspection interval

RESULTS

Figure 4: Two options of a damage tolerance analysis of a railway axle.

2.2 Configurations Investigated Within This Study

As mentioned in section 1 the aim of this study was a systematic investigation of factors which potentially influence the residual lifetime of an axle. That means on the other hand that no exact numbers will be given, e.g., for residual lifetimes of individual axle configurations since these are not necessary for identifying the trends. Figure 5 gives an overview on the configurations dealt with. These comprised three hollow and one solid axle made of two

different materials (A1 and A4). The crack positions were at the V transition, at the T transition, at the wheel press fit and at the shaft away from stress concentrations and press fits. Four loading sequences were applied which were given as bending moments σ_b at the shaft position or as forces Q_1 , Q_2 , Y_1 and Y_2 such as illustrated in Figure 5. They were provided as sequences of loading blocks or individual cycles or as load spectra and they referred to high speed traffic as well as to the traffic at a curved track.

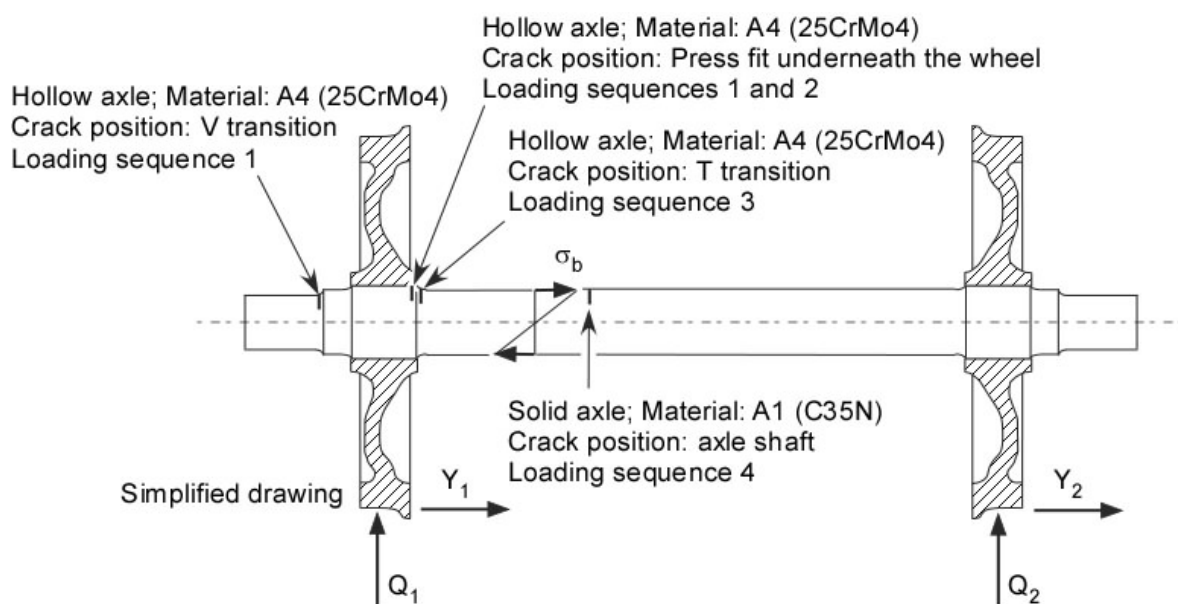


Figure 5: Overview on the axle configurations investigated in the present study.

2.3 Fracture Mechanics Analyses

The general scheme of the fatigue crack propagation analyses is illustrated in Figure 6. It is important to perform separate analyses for the centre and the surface points (A and B) of the semi-elliptical surface crack, i.e., the crack has to be allowed to vary its depth-to-length ratio during propagation. The failure criteria chosen in the present analyses were the wall

breakthrough of the crack in the hollow axles and a crack depth-to-axle radius ratio of 0.9 in the solid axle. In any case the maximum K value, K_{\max} , of the loading cycle referring to the highest loading amplitude was well below the fracture toughness of the material. If the ligament yielding prior to axle failure exceeds a certain limit (usually given by a ligament yielding parameter $L_r = 0.5$ with L_r being the ratio between a net section reference stress and the yield strength of the material) ligament yielding correction of the crack driving force has to be carried out. This is indicated by (*) in Figure 6. No detailed discussion of this point is given here; instead the reader is referred to [14].

Note that a failure criterion such as the wall breakthrough of the crack instead of axle fracture might be significantly conservative with respect to the critical crack depth. It is, however, only slightly conservative with respect to the residual lifetime. This is because the crack propagation rate of relatively large cracks is so high that failure is imminent whatever the actual crack size.

For each load level stress intensity factor values ΔK had to be determined. This was done by using available analytical K factor solutions in two cases: the hollow axle with the crack position at the V transition [15] and the solid axle with the crack position at the axle shaft away from stress concentrations and press fit locations [16]. In the two other cases K factor solutions were derived by Finite Element analyses for a number of predefined crack depths, a , and depth-to-half surface length ratios, a/c . Two examples of Finite Element meshes are given in Figure 7. The numerically derived K factor solutions were then used analytically in the subsequent analyses. All K factor solutions used by the authors for railway axles are recorded in the K factor compendium within this issue [17].

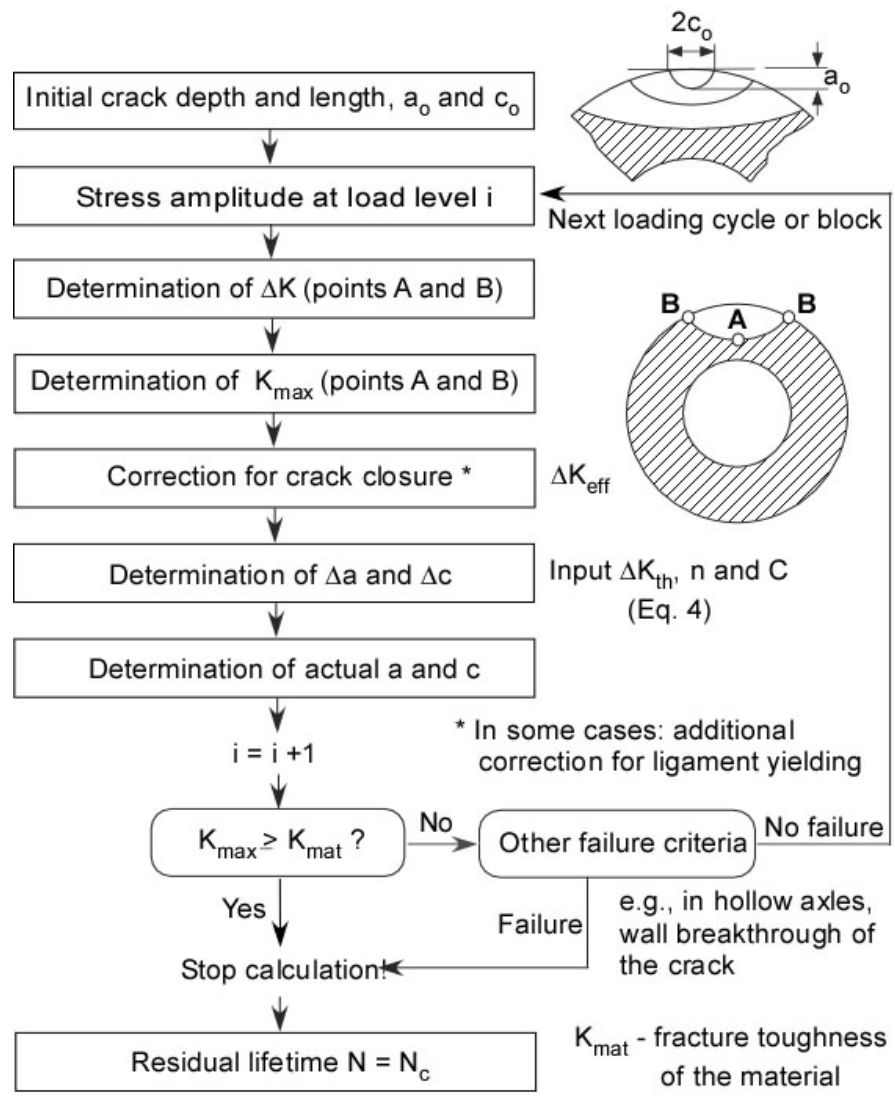


Figure 6: Scheme of a fatigue crack propagation analyses of a railway axle.

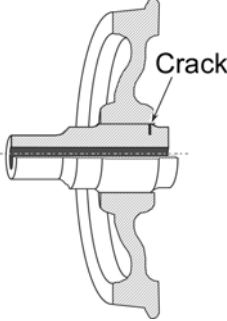
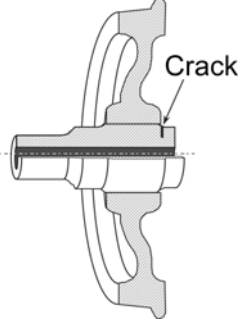
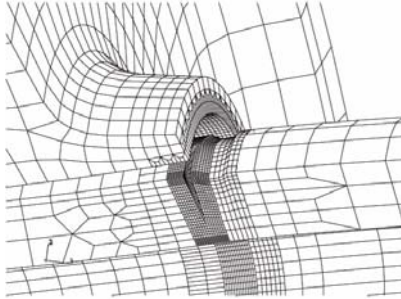
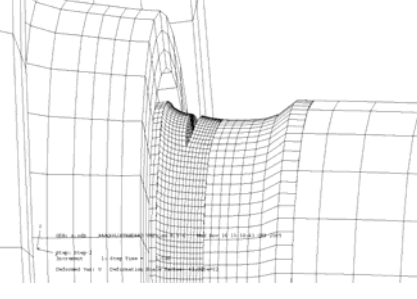
Crack position	at wheel press fit	at T transition
Drawing		
Finite Element mesh		

Figure 7: Finite element meshes for determining stress intensity factor solutions for a crack at the press fit beneath the wheel and a crack at the T transition.

The numerical K factor solutions comprised solutions for the centre and surface points A and B (see Figure 6) of the crack, for the loading components F_H , F_{V1} , F_{V2} and for the press fit loading. The equations correlating these forces with the input loading components Q_1 , Q_2 , Y_1 , Y_2 and σ_b (Figure 5) are provided in [17]. Besides mode I they also include mode II and mode III solutions. In one case, the crack at the T transition (see Figure 5 and Figure 7 right), plane and rotating bending was simulated (see section 3.2.3).

The determination of ΔK values required K factor solutions for the minimum and maximum bending moments, K_{\min} and K_{\max} , within one loading cycle. These were provided by simulating 6 and 12 o'clock positions of the wheel such as illustrated in Figure 8 with K_{\max} referring to K at the 12 o'clock position and K_{\min} referring to K at the 6 o'clock position.

First the ΔK components for modes I, II and III, ΔK_I , ΔK_{II} and ΔK_{III} , were separately determined. Then the mixed mode equivalent cyclic stress intensity factor ΔK_v was obtained by

$$\Delta K_v = \frac{\Delta K_I}{2} + \frac{1}{2} \sqrt{(\Delta K_I)^2 + 4 \cdot (1.155 \Delta K_{II})^2 + 4 (\Delta K_{III})^2} \quad (2)$$

[18]. Within this equation the ΔK_I values were corrected for crack closure using Newman's approach [19]

$$\Delta K_I \rightarrow \Delta K_{\text{eff}} = \left(\frac{1-f}{1-R} \right) \Delta K_I \quad (3)$$

No detailed discussion on this topic will be given here, see, however [7] and [20]. The parameter α necessary for determining the crack closure function f such as recommended in [21] for steels was assumed to be 2.5.

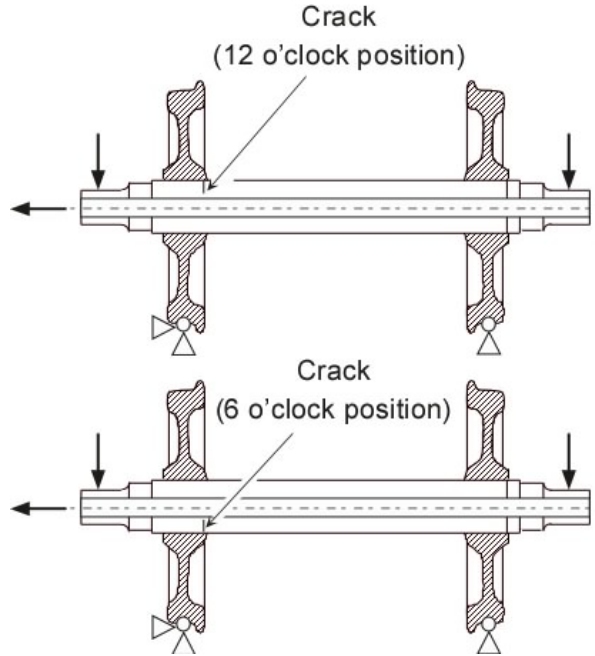


Figure 8: The 12 and 6 o'clock positions referring to the maximum and minimum bending moments within one loading cycle.

3. PARAMETERS INFLUENCING THE RESIDUAL LIFETIME OF AXLES WITH FATIGUE CRACKS

3.1 Material Parameters

3.1.1 Fatigue crack propagation characteristics (da/dN- ΔK curve)

The most important material property needed for a damage tolerance analysis is the fatigue crack propagation characteristics, i.e., the $da/dN-\Delta K$ curve. Figure 9 shows the data of five tests on A4 (25CrMo4) steel carried out for R ratios ($R = K_{min}/K_{max}$) of 0.1 (two tests), 0.5 (two tests) and -1 (one test). All data have been corrected for crack closure using Eq. (3). In addition the BSI 7910 [22] reference curve for steels operating in air

$$\frac{da}{dN} = C \cdot \Delta K^n \quad (4)$$

($C = 5.21 \times 10^{-13}$ and $n = 3$ with da/dN being in mm/cycle and ΔK being in $\text{MPa}\sqrt{\text{mm}}$)

is plotted into the diagram. As can be seen this curve provides an adequate upper bound to the experimental data in the Paris range of the $da/dN-\Delta K_{\text{eff}}$ curve. This is because the crack growth rates for steel in that range are in general little affected by the material grade. The subsequent analyses are based on the BSI 7910 data and not on the experimental results.

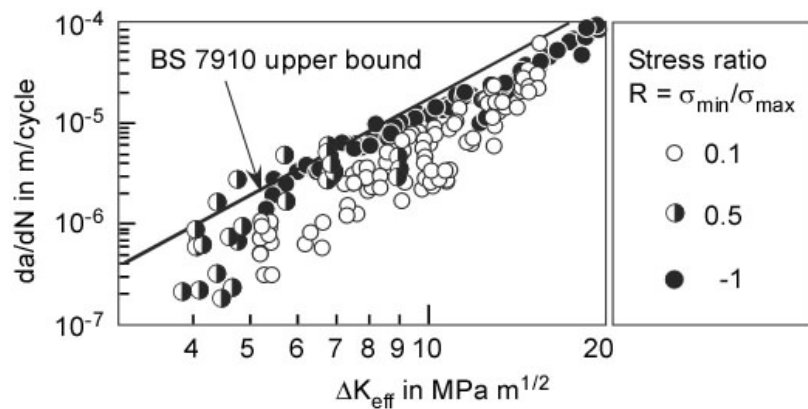


Figure 9: The data of 5 $da/dN-\Delta K_{\text{eff}}$ curves of the steel A4 determined for three R ratios ($R = 0.1, 0.5$ and -1) in comparison with the BS7910 upper bound reference curve (Experimental data: P. Hübner).

For design purposes usually an upper bound curve to the $da/dN-\Delta K$ data has to be applied. The alternative is to perform a statistical analysis. A method for statistically processing the $da/dN-\Delta K$ data based on the fit parameter C in Eq. (4) is presented in [23]. Applying it to the data of Figure 9 provides the crack depth vs. number of cycle curves shown in Figure 10. As

can be seen the difference in residual lifetimes between a 95% upper and a 5% lower bound of C is almost a factor of three. Note that the data refer to one batch. Taking into account axles from various batches and manufacturers would certainly further increase the scatter.

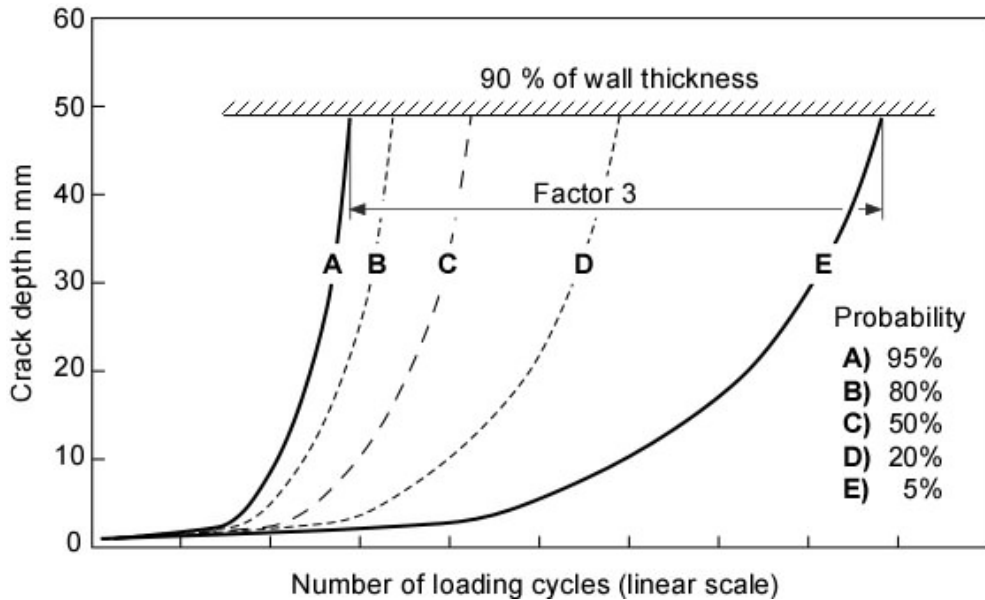


Figure 10: Crack depth vs. number of cycle curves for different percentile values of the fit parameter C in Eq. (4); hollow axle, crack position at the T position.

3.1.2 Toughness

It was already mentioned in section 2.3 that the precise value of the final crack size at fracture is not particularly important with respect to residual lifetime because the large crack is propagating so rapidly that there is little effect of different critical crack sizes on the residual lifetime. In other words: The major part of the residual lifetime is consumed during the early extension of the small initial crack and not at the final stage prior to fracture. With respect to the fracture toughness of the material a similar statement has to be made. In the present study it was consistently found that the maximum K_{\max} value (referring to the highest stress

amplitude) at failure, i.e. the wall breakthrough of the crack was well beyond the 5% percentile value of the fracture toughness. At that time the crack already grew so rapidly that not much additional lifetime could be expected after the breakthrough.

This statement is insofar important as it is sometimes argued that higher fracture toughness values may compensate the increased stresses due to smaller wall thicknesses in “light-weight” hollow axles made of higher strength steels. This, as a rule, is not true, at least not with respect to the residual lifetime of an axle. Almost a decade ago Benyon and Watson made the following statement [5]: “Manufacturers often consider using higher strength axle steels to achieve higher allowable stresses...However, crack growth rates for steel are in general unaffected by material grade. This means that higher operation stresses will lead to increased defect growth rates, leading in turn to shorter inspection periodicities...Relatively modest changes in stress level have a significant influence on the inspection interval. A 10% increase in stress level reduces the inspection interval by a factor of between 2 and 3.”

Any reduction of the wall thickness of a hollow axle without reducing the weight of the complete vehicle has two effects: the stresses across the wall are increased (with the effect described above) and, additionally, the possible distance for the fatigue crack to grow is reduced. Both effects cause significant reduction of the residual lifetime and – proportionally to this – substantial shortening of the inspection interval. This should always be kept in mind when railway axles are planned be optimised with respect to their weight.

3.1.3 Fatigue Crack Propagation Threshold ΔK_{th}

A special problem refers to uncertainties in the long fatigue crack propagation threshold ΔK_{th} (for definition see Figure 3, top right). The basic principle is straightforward: For crack

driving forces ΔK in the component smaller than ΔK_{th} no crack propagation occurs. In contrast crack propagation always takes place for $\Delta K > \Delta K_{th}$. However, in reality ΔK_{th} shows some scatter. Investigating this on A1N axle steel the authors of [24] identified a value of $\Delta K_{th} = 7.39 \pm 0.86 \text{ MPa}\sqrt{\text{m}}$ for $R = 0$ based on Gaussian distribution. The problem becomes confusing when the axle, as is commonly the case, is loaded by variable amplitudes. In that case the loading cycles with larger amplitudes could contribute to crack propagation whereas smaller amplitude cycles would not. Since the cyclic stress intensity factor ΔK , in contrast to the cyclic stress $\Delta\sigma$, increases with the crack size the question whether a loading cycle contributes to crack extension or not also depends on the crack depth. This is illustrated by Figure 11 where a sequence of 11 loading blocks is repeatedly applied to the axle with the crack at the V transition. Let us assume a ΔK_{th} value of $2.5 \text{ MPa}\sqrt{\text{m}}$. At a crack depth of 1.5 mm only the loading block with the highest amplitude (block 1) contributes to crack propagation. When the crack is growing loading blocks with smaller amplitudes become active too, i.e., block 4 from a crack depth of about 2.5 mm. Finally, at a crack depth of about 13 mm all loading blocks including block 11 with the lowest amplitude push the crack forward.

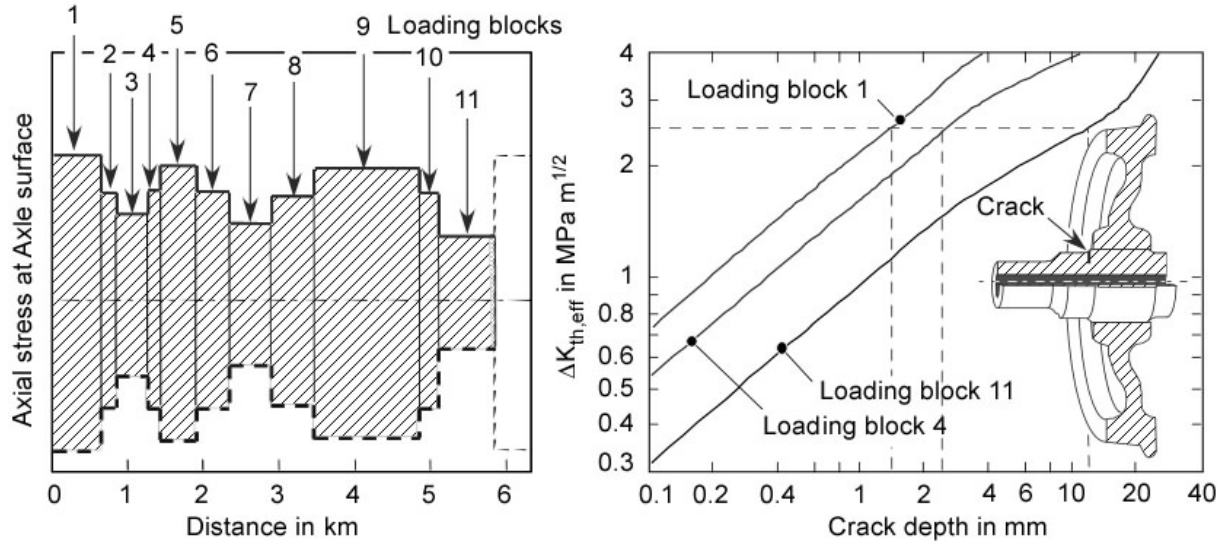


Figure 11: Crack sizes at which loading blocks of different amplitudes become active in terms of crack propagation; hollow axle, crack position at the V position (Analysis: C. Andersch [7]).

This effect is relevant because the intrinsic fatigue crack propagation threshold in steels (corresponding to $\Delta K_{th,eff}$) is in the order of 2.4 to $2.6 \text{ MPa}\sqrt{\text{m}}$ [25]. If we take into account a scatter in ΔK_{th} in the order reported above we end up with a significant uncertainty in the residual lifetime analysis. Figure 12 provides an example of how the difference between threshold values of 2 and $3 \text{ MPa}\sqrt{\text{m}}$ can affect the predicted residual lifetime of an axle. Compared to a curve without threshold ($\Delta K_{th} = 0$, the Paris line is extended to the left) the residual lifetime is increased by about 18% for $\Delta K_{th} = 2 \text{ MPa}\sqrt{\text{m}}$, however, it becomes larger by orders of magnitude for $3 \text{ MPa}\sqrt{\text{m}}$. In order to bypass this problem the authors applied a threshold value of $\Delta K_{th} = 2 \text{ MPa}\sqrt{\text{m}}$ as it is recommended for steels in BS 7910 [22] in this study. Note, however, that the consequence might be very high conservatism, a problem which is not at all solved so far.

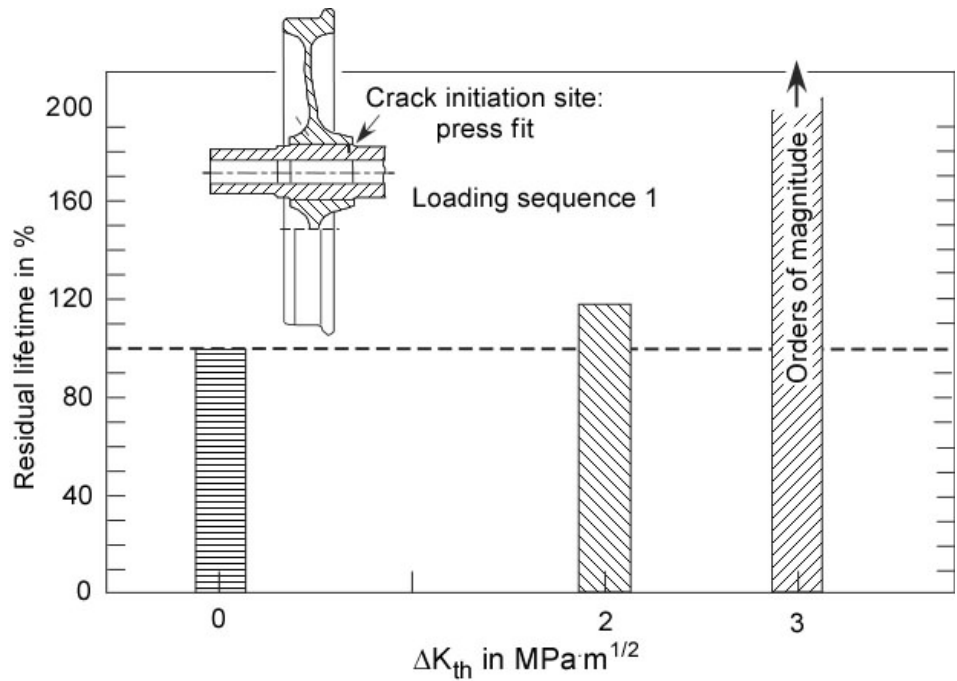


Figure 12: Effect of the fatigue propagation threshold on residual lifetime; hollow axle with crack position at the wheel seat press fit; variable amplitude loading.

3.2 Loading

3.2.1 General comments

In section 3.1.2 Benyon and Watson were cited with the statement that a 10% increase in the stress level would reduce the inspection interval, which is proportional to the residual lifetime of the component, by a factor of 2 or 3. The reason for this sensitivity is provided by Eq. (4) where the crack propagation rate da/dN correlates exponentially ($n = 3$) with the cyclic stress intensity factor ΔK . Since ΔK is linearly proportional to the load that means

$$N_c \square \frac{1}{\Delta\sigma^3} \quad (5)$$

with N_c being the number of loading cycles at failure and σ the applied stress. As a consequence of the load sensitivity of the residual lifetime the loading of the axle has to be specified with high accuracy which usually requires numerical (multi-body) simulation as well as measurements under service conditions in addition to the common design rules such as reproduced for various railroad systems in [26]. As an illustration of the effect of axle loading North American railroad experience with axle failures in freight cars can be cited. Whilst the number of axle failures with two or three failure events per year was small before 1995 it increased significantly after that time up to 4 events in 1998, 7 events in 1999, 2000 and 2001 and even 27 events in 2002 [27]. The authors of [27] identified the reason for this development in the fact that the permissible in-service load was allowed to be increased by 10% after 1995.

The loads an axle is subjected to can be partitioned in bending and axial tension and in primary and secondary components. The bend loading is due to the weight of the vehicle amplified by dynamic effects. Note that these can be further increased by irregularities such as out-of round wheels or corrugated rails. The axial loading component is due to cornering at curved tracks and impacts at crossovers or switches. Tilting trains are sometimes subjected to increased axial forces particularly if the track is characterised by small-radius curves and local track irregularities [28]. All these loading components are primary. The secondary loading is induced by the press fits. These do not affect the cyclic stress intensity factor $\Delta K = K_{max} - K_{min}$ but the R ratio, $R = K_{min}/K_{max}$. Note that ΔK as well as R show different values along the front of the semi-elliptical surface crack. Therefore, for a damage tolerance analysis, a meaningful definition of the R ratio can only be based on the stress intensity factor and not, as it is common in fatigue strength concepts, on the global stresses.

3.2.2 Press fit loading

The deformation pattern and stress field due to the wheel and gear press fits in a hollow axle is illustrated in Figure 13. Whereas the local loading beneath the press fit is characterised by compression it is local tension at the surface of the adjacent geometrical transitions, e.g., at the T transition.

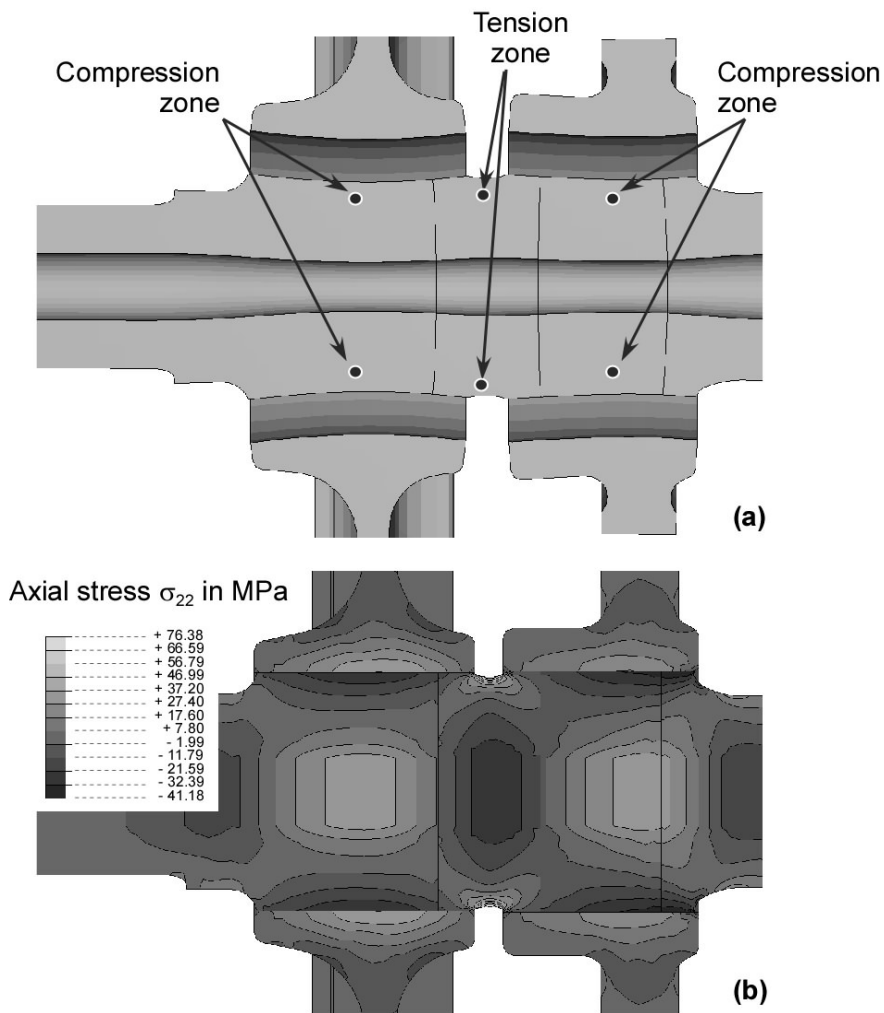


Figure 13: Press fit loading of a railway axle. (a) Deformation pattern and (b) stress distribution (according to [20]).

In order to investigate the effect of the wheel press fit on the residual lifetime Finite Element analyses were performed. The contact problem was solved by applying the interference fit method [29] which is based on a master-slave contact type, the main parameter of which is a user specific “interference value” between wheel and axle. This way, simulations were carried out for both the maximum and the minimum press fit tolerances in design. The behaviour in tangential direction was based on the classical Coulomb approach, i.e. the maximum allowable shear stresses were related to the contact pressure due to the press fit. The friction coefficient was chosen as $\mu = 0.6$. For more details see [20]. The analyses were carried out for variable amplitude loading.

The results of the analyses are shown in Figure 14. Whereas the initiation of the crack is caused by fretting underneath the wheel seat its propagation is interfered by the compression stress field which the crack has to pass (Figure 13). As a consequence the lifetime of the wheel press fit crack, compared to the case without press fit, was found to be extended by about 50 and 60% for the two loading sequences investigated. In contrast, press fitting was found to be detrimental for the T transition crack. Because the press fit causes a tension stress field (Figure 13) at that position crack propagation was accelerated and the residual lifetime was reduced to about one third compared to the analyses not considering the press fit effect.

Madia et al. [20], investigating the press fit effect on the T transition crack in another hollow axle geometry subjected to constant amplitude loading, even found a reduction in residual lifetime of a factor 4.2. The results clearly indicate that the T transition, compared to the wheel press fit crack, is the more critical position with respect to damage tolerance. In order to adequately describe this case the detrimental press fit effect has to be taken into account by proper modelling the contact problem.

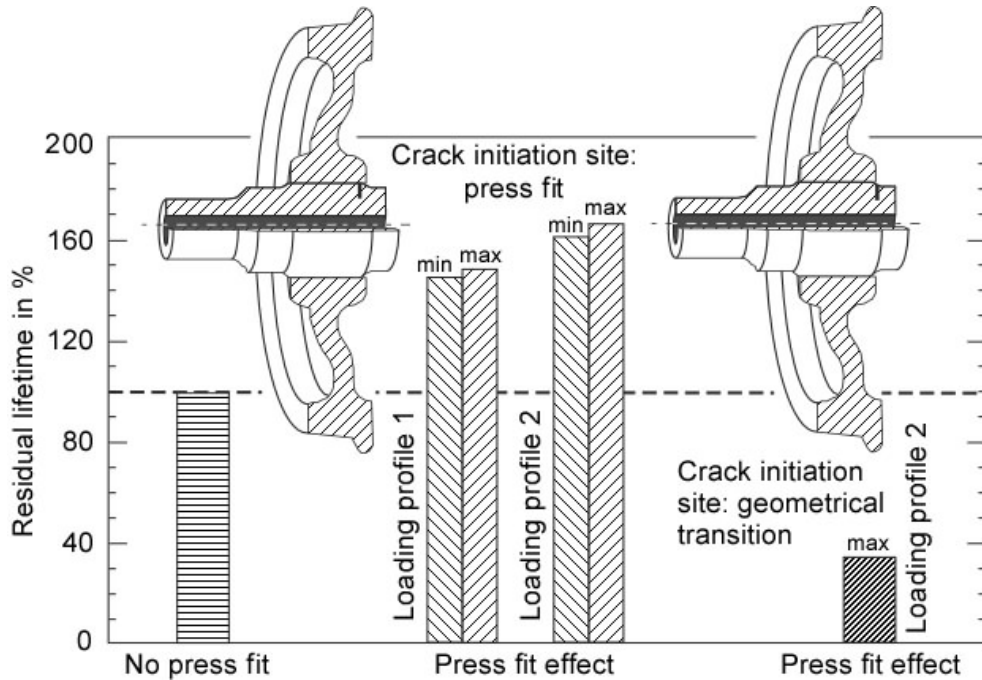


Figure 14: Effect of the wheel press fit on the residual lifetime; hollow axle; crack positions underneath the wheel seat and at T transition; variable amplitude loading. The subscripts “min” and “max” refer to the tolerance limits of the press fit.

3.2.3 Plane vs. rotating bending

Usually, K factor solutions for cylinders are available for plane bending while railway axles are subjected to rotating bending. There are a few exceptions for solid and thick-walled hollow cylinders, however, without geometrical transitions [30,31]. In [20] Madia et al. modified the model in [31] for a hollow railway axle. The question to be answered in this section is how big the error in residual lifetime will be when the analysis is based on plane instead of rotating bending. For this, K factor solutions were derived for both loading geometries (see [17]). The principle is illustrated in Figure 15. Whereas the centre line of the surface crack is always in the 12 o’clock position for plane bending it is only in the 12 o’clock position for determining K_A at the deepest point but is turned to the side for determining K_B at

the surface point for rotating bending. The degree of rotation depends on the crack dimensions since it was chosen such that the surface point in each case was put to the 12 o'clock position.

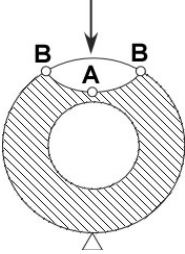
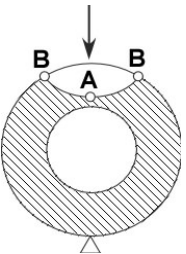
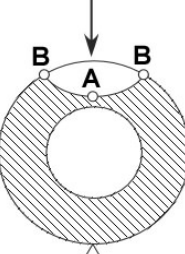
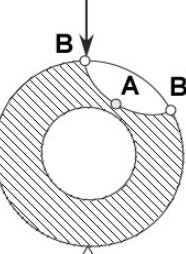
Loading type	K_A (Stress intensity factor at the deepest point)	K_B (Stress intensity factor at the surface points)
Plane bending		
Rotating bending		

Figure 15: Determination of the stress intensity factor at the deepest and the surface points of the crack for plane and rotating bending.

By performing the investigation for the hollow axle with the crack at the T position and variable amplitude loading the rotating bending effect was found to be rather small. The residual lifetime of the axle was about 4% smaller than that of the axle loaded by plane bending. Madia et al. [20], performing a similar analyses for an axle subjected to constant

amplitude loading, found an even smaller difference of about 1 %. The reason for the difference is that the propagation of the crack at the surface is slightly faster in rotating than in plane bending due to a slightly higher K_B value (Figure 16). Note, however, that the effect is negligible compared to that of other factors such as material scatter or applied and press fit loads.

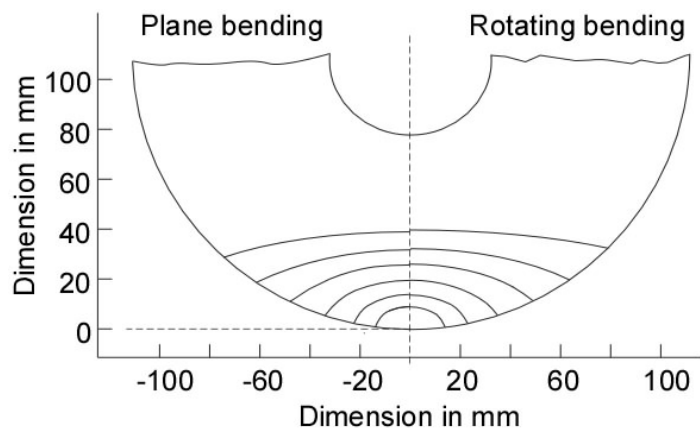


Figure 16: Simulation of crack extension in a hollow axle subjected to plane (left) and rotating bending (right).

3.2.4 Mixed mode loading

Analytical stress intensity factor solutions are usually exclusively based on mode I considerations. However, the semi-elliptical surface crack in a press fitted axle is subjected to mode II and III loads as well. The solutions for the hollow axles with cracks at the press fit underneath the wheel seat and at the T transition, therefore, were generated to include mode II and III components. This raises the question about the error a residual lifetime analyses causes which does not consider mixed mode. In Figure 17 the result is presented for the wheel press

fit crack. For the two loading sequences investigated the over-prediction of residual lifetime was found to be 23 and 26% when the mixed mode contribution to the crack driving force was neglected. This is significant but still small compared to the effect of the other parameters investigated within this study and can probably be covered by a safety margin on the residual lifetime. However, further investigations seem to be necessary at that point.

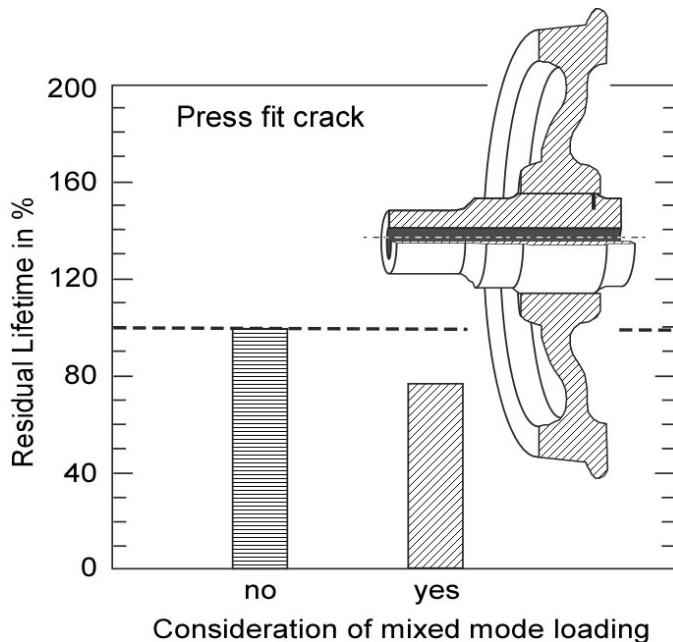


Figure 17: Effect of considering and not considering the mixed mode loading components on the residual lifetime; hollow axle; crack position underneath the wheel seat; variable amplitude loading.

3.2.5 Load history effects

Load history or interaction effects occur when a constant amplitude cyclic loading is interrupted by an overload or a number of overloads. It is well known that tensile overloads can cause crack retardation whereas compression overloads can cause crack acceleration this way extending or reducing the residual lifetime (see [32] in this issue). Load history effects

can also occur when the loading amplitude is not basically constant but varying. Neglecting potential load history effects would lead to conservative predictions in case of tensile overloads but to non-conservative ones in case of compression overloads. Note, however, that, in real applications, tensile and compression overloads can also level out this way having no substantial effect on residual lifetime.

Within this study the potential load history effect was investigated for the hollow axle with the crack at the V transition. For doing so the FASTRAN program [33] was used. The results were then compared with an analysis not considering the effect. For the method applied see also [7]. The results are given in Figure 18 for the loading block sequence according to Figure 11. Almost no effect is found in this specific case. Similar results were obtained by the authors of [34] for a high-speed traffic loading sequence. Note, however, that other authors disagree with this conclusion based on their own investigations of railway axles [35]. What might be important is, that the results in Figure 18 were obtained for a $da/dN-\Delta K$ curve without threshold ($\Delta K_{th} = 0$).

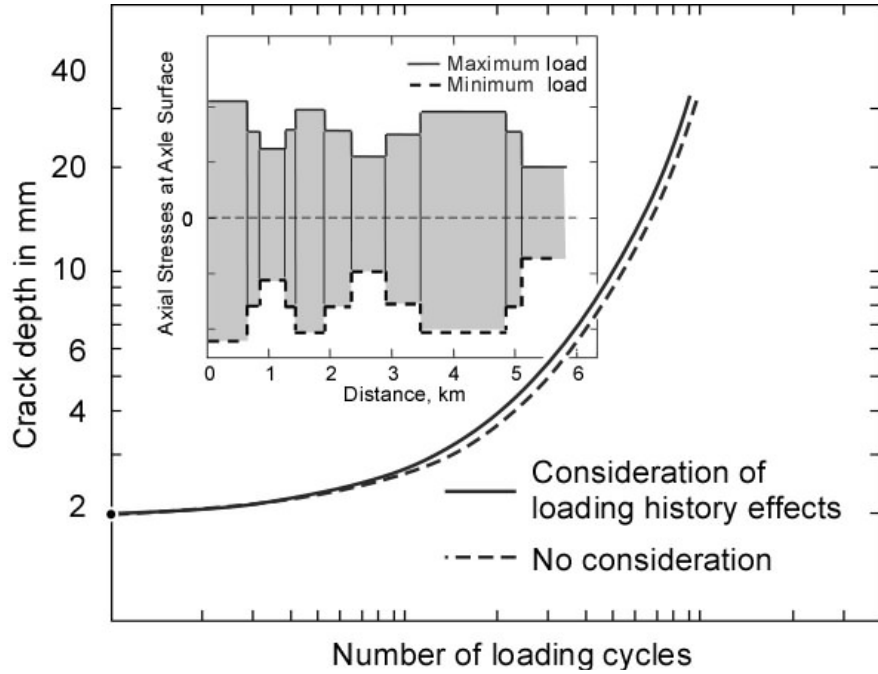


Figure 18: Comparison of crack depth vs. number of loading cycle curves considering and not considering potential load interaction effects; hollow axle with the crack at the V transition (Analysis: C. Andersch [7]).

3.3 Initial crack geometry a_0/c_0

The final parameter investigation in this section was already published in [20] and shall only be briefly summarised here. The simulations above were all based on a semi-circular initial crack $a_0/c_0 = 1$. In the following the residual lifetime of a hollow axle with a crack at the T transition for initial crack ratios of $a_0/c_0 = 1$ and 0.2 will be compared. The initial crack depth a_0 was identical in both cases ($a_0/t = 0.02$). As expected the residual lifetime of the $a_0/c_0 = 1$ crack was the larger one. However, the difference was in the order of only 20% (Figure 19). The main difference in crack propagation occurred at the early stage. Note that other options

such as multiple cracks at different positions around the circumference are not considered so far. This should certainly be investigated in a future activity.

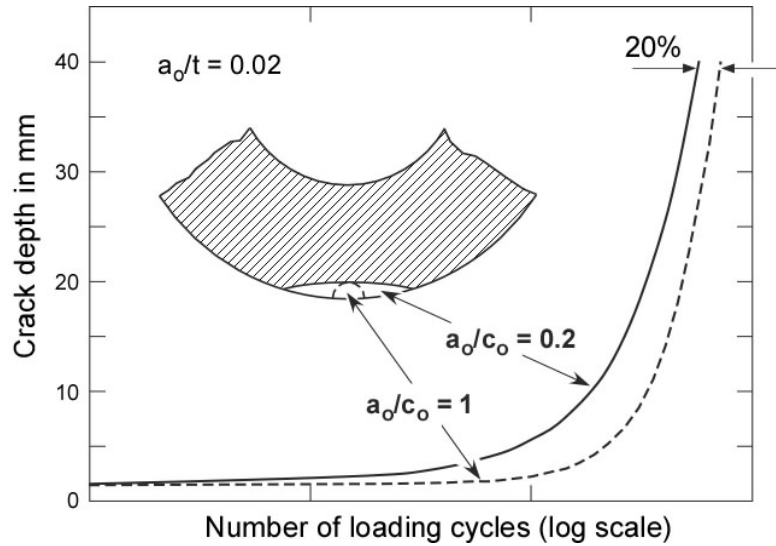


Figure 19: Crack depth vs. number of loading cycle curves for initial crack geometries $a_0/c_0 = 1$ and 0.2 but identical initial crack depths a_0 ; hollow axle with the crack at the T transition.

4. Summary

The damage tolerance approach assumes the existence of a fatigue crack which potentially can grow to its critical size during the projected lifetime, this way causing failure of the component. In order to avoid such a scenario the crack has to be detected in due time by regular non-destructive inspections. The aim of a damage tolerance analysis is to provide the operator with information either on the required inspection interval or on the minimum crack size which has to be detected for an existing inspection interval. The basic information for both options is the so-called residual lifetime which is the time or number of loading cycles an

initial crack needs to extend up to failure. In that context the size of the initial crack refers to the limitations of the non-destructive inspection technique applied. A crack that could be missed during an inspection under in-service conditions is postulated to exist.

The aim of the present paper was to perform a systematic investigation of various parameters influencing the residual lifetime. These comprised material data as well as the loading characteristics and the initial crack geometry.

The relevant material data for determining the residual lifetime of a railway axle are the fatigue crack propagation characteristics, i.e., the $da/dN-\Delta K$ curve and the fatigue threshold ΔK_{th} . Investigating the scatter in $da/dN-\Delta K$ of an axle steel the authors found that it corresponded to a variation in residual lifetime of a factor of 3. The upper bound was, however, adequately described by the reference curve according to the standard BS 7910.

The ΔK_{th} value including scatter was identified to be problematic for the analysis because the residual lifetime sensitively responded to even small variations in ΔK_{th} . The authors bypassed this problem by conservatively choosing $\Delta K_{th} = 2 \text{ MPa}\sqrt{\text{m}}$ such as recommended by BS 7910 for steels. It can, however, not be excluded that this choice could generate unnecessary conservatism in practical application. Further investigations are needed here.

The fracture toughness of the material was demonstrated not to be of major importance for the damage tolerance of railway axles because it is of little effect on the residual lifetime due to the rapid propagation of the crack during its final stage. It was discussed, in that context, that the detrimental effect of a reduction in wall thickness of a hollow axle on residual lifetime and inspection interval therefore cannot be compensated by improved fracture toughness values.

The loading parameters investigated were the press fit effect, rotating vs. plane bending, load history of variable amplitude loading and the mixed mode components of the crack driving force.

The most remarkable results were obtained for the press fit effect due to which additional compressive and tension stresses are generated at the axle surface underneath the wheel, gear or disk brake seats and at the geometrical transitions adjacent to the press fit regions, respectively. Comparing the residual lifetimes of a crack growing underneath the wheel seat and at the T transition the authors found it to be increased by about one half for the first one but reduced by a factor of 3 (!) for the latter one. The T transition was clearly identified to be the more critical crack site. The tremendous detrimental effect of the press fit on the residual lifetime at this site emphasizes the importance of appropriate modelling the contact problem of the press fits.

A less considerable effect was found with respect to mixed mode loading. When, as it is common practice of analytical K factor solutions, the mode II and III loading components were neglected the resulting lifetime prediction was non-conservatively wrong by about one quarter. The authors think that this, if necessary, could be compensated by a safety margin the order of which should, however, further substantiated by additional investigations.

A negligible effect of 4% difference in residual lifetime was found when the analysis was carried out assuming plane instead of the realistic rotating bending loading. There was also no indication of a pronounced load history effect for the investigated axle configuration.

Assuming two different initial crack shapes ($a_0/c_0 = 1$ and 0.2) but an identical initial crack depth a_0 , a difference in residual lifetime of about 20% was found. This shows that there is some effect of the initial crack configuration which could also refer to further options such as

multiple cracks around the axle's circumference which, however, were not subject of the present study. Certainly further work is needed for this topic.

References

- [1] Smith, R.A. and Hillmansen, S. (2004): A brief historical overview of the fatigue of railway axles. Proc. Instn. Mech. Engrs. Vol. 218, Part F: J Rail and Rapid Transport, 267-274.
- [2] Smith, R.A. (1998): Fatigue in transport: Problems, solutions and future threads. Proc. Proc. Instn. Chem. Engrs. Vol. 76, Part B, 217-223.
- [3] Sakai, T., Ochi, Y. and Jones, J.W. (2006): Third International Conference on Very High Cycle Fatigue (VHCF-3), Kyoto/Kusatsu, Japan. Int. J. Fatigue 28, Issue 11.
- [4] Gravier, N. Viet, J.-J. and Leluan, A. (1998): Predicting the life of railway vehicle axles. In: Weixing, H. (ed.), Proceedings of the 12th Int. Wheelset Congress , Quigdao, China, 133-146.
- [5] Benyon, J.A. and Watson, A.S. (2001): The use of Monte-Carlo analysis to increase axle inspection interval. Proceedings of the 13th Int. Wheelset Congress , Rome, Italy.
- [6] Beretta, S., Carboni, M., Lo Conte, A. and Palermo, E. (2008): An investigation of the effects of corrosion on the fatigue strength of A1N axle steel. Proc. Instn. Mech. Engrs. Vol. 222, Part F: J Rail and Rapid Transport, 129-143.

[7] Zerbst, U., Vormwald, M., Andersch, C., Mädler, K. and Pfuff, M. (2005): The development of a damage tolerance concept for railway components and its demonstration for a railway axle. Engng. Fracture Mech. 72, 209-239.

[8] Rudlin, J.R. and Shipp, R. (2002): Review of techniques for rail axle inspection. Report for railway safety; also Rudlin, J.R. and Shipp, R. (2003): Review of rail axle inspection methods. Int. Seminar on Fatigue of Axles, Imperial College London, 25-26 September 2003.

[9] Beretta, S., Carboni, M., Rudlin, J. And Wei, L. (2009): Damage tolerance and design review for the axles of a high speed train. Engng. Fracture Mech, [This issue](#).

[10] Carboni, M., Cantini, S. and Beretta, S. (2009): Analysis and determination of UT POD curves for railway axles. Engng. Fracture Mech, [This issue](#).

[11] Carboni, M. and Beretta, S. (2007): Effect of probability of detection upon the definition of inspection intervals for railway axles. Proc. Instn. Mech. Engrs. Vol. 221, Part F: J Rail and Rapid Transport, 409-417.

[12] Hansen, W. and Hintze, H. (2002): Ultrasonic testing of railway axles with phased array technique. NDTnet, Vol. 7, No. 10, www.ndt.net/article/ecndt02/108/108.htm.

[13] Hands, G. (1996): Automated NDT. Advantages and disadvantages. NDTnet, Vol. 1, No. 03, www.ndt.net/article/hands/hands.htm.

[14] Zerbst, U., Schödel, M., Webster, S. und Ainsworth, R.A. (2007): Fitness-for-Service Fracture Assessment of Structures Containing Cracks. A Workbook based on the European SINTAP/FITNET Procedure. Elsevier-Verl., Amsterdam et al..

[15] Chapuliot, S. (2000) : Formulaire der K_I pour les tubes comportant un défaut de surface semi-elliptique longitudinal ou circonférentiel interne ou externe. Commissariat à l' Énergie Atomique (CEA), Saclay, CEA-R-5900.

[16] Levan, A. und Royer, J. (1993): Part-circular surface cracks in round bars under tension, bending and twisting. Int. J. Fracture 61, 71-99.

[17] Madia, M., Beretta, S., Schödel, M., Zerbst, U., Varfolomeyev, I. and Luke, M. (2009): Stress intensity factor solutions for railway axles. Engng. Fracture Mech, [This issue](#)

[18] Richard, H.A. (2003): Festigkeitsnachweis unter Mixed-Mode-Bbeanspruchung. Materialprüfung 45, S. 513-18.

[19] Newman, J.C., Jr. (1981): A crack-closure model for predicting fatigue crack growth under random loading. ASTM STP 748, 53-84.

[20] Madia, M., Beretta, S. and Zerbst, U. (2008): An investigation on the influence of rotary bending and press fitting on stress intensity factors and fatigue crack growth in railway axles. Engng, Fracture Mech. 75, 1906-1920.

[21] NASGRO: Fatigue Crack Growth Computer Program „NASGRO“, Version 3. NASA, L.B. Johnson Space Centre, Houston, Texas. JSC-22267B, 2000.

[22] BS 7910 (2005): Guide on Methods for Assessing the Acceptability of Flaws in Metallic Structures. British Standard Institution. Section 8.2.3.5.

[23] Hübner, P., Zerbst, U. Berger, M. and Brecht, T. (2009): The Fracture of a wobbler in a heavy plate mill. Engng. Failure Analysis. In press.

[24] Beretta, S. and Carboni, M. (2006): Experiments and stochastic model for propagation lifetime of railway axles. Engng. Fracture Mech. 73, 2627-2641.

[25] Hardboletz, A., Weiss, B. and Stickler, R. (1994): Fatigue thresholds of metallic materials. In: Carpenteri, A. (ed.): Handbook of Fatigue Crack Propagation in Metallic Structures. Elsevier, 847-882.

[26] Hirakawa, K., Toyama, K. and Kubota, M. (1998): The analysis and prevention of failure in railway axles. Int. J. Fatigue 20, 135-144.

[27] Lonsdale, C. and Stone, D. (2004): North American axle failure experience. Proc. Instn. Mech. Engrs. Vol. 218, Part F: J Rail and Rapid Transport, 293-298.

[28] Gasemyr, H. and Ly, J.N. (2002): Beurteilung des Einflusses der Gleislagequalität in Gleisbögen mit kleinen Radien auf die Beanspruchung an Radsatzwellen der Drehgestelle für Neigezüge am Beispiel eines durchgeföhrten Messprogramms in Norwegen. ZEVrail Glasers Annalen – 126 Tagungsband SFT Graz.

- [29] ABAQUS®. Ver 6.5.3 Reference Manual. 2005.
- [30] de Freitas, M. and Francois, D. (1995): Fatigue crack growth in rotary bend specimens and railway axles. Engng. Materials and Structures 18, 171-178.
- [31] Carpenteri, A., Brighenti, R. and Spangnoli, A. (2000): Fatigue growth simulation of part-through flaws in thick-walled pipes under rotary bending. Int. J. Fatigue 22, 1-9.
- [32] Sander, M. and Richard, H.A. (2009): Investigations on fatigue crack growth under variable amplitude loading in wheelset axles. Engng. Fracture Mech, [This issue](#).
- [33] Newman, J.C., Jr. (1992): FASTRAN II – a fatigue crack growth structural analysis program. NASA-TM 104159.
- [34] Beretta, S. and Carboni, M. (2004): Simulation of fatigue crack propagation in railway axles. ASTM STP 1641, 368-381.
- [35] M. Sander, M. and H.A. Richard, H.A. (2009): Investigations of fatigue crack growth in wheelset axles. 2nd Int. Conference Material and Component Performance under Variable Amplitude Loading, Darmstadt, Germany, March 23-26, In press.

Nomenclature

a	crack depth
a_0	initial crack depth to be postulated as existing in a damage tolerance analysis
a_d	crack depth which has to be detected depending on the inspection interval
A	deepest point of the semi-elliptical surface crack
B	surface points of the semi-elliptical surface crack
c	half crack length at surface
c_0	initial half crack length to be postulated as existing in a damage tolerance analysis
C	fit parameter of Eq. (4)
da/dN	fatigue crack propagation rate
f	crack closure function (Eq. 3)
IA	inspection interval
K	linear elastic stress intensity factor (K factor)
K_I, K_{II}, K_{III}	mode I, II and III stress intensity factors
K_A	K factor at the deepest point (A) of the semi-elliptical surface crack
K_B	K factor at the surface points (B) of the semi-elliptical surface crack
K_{mat}	fracture toughness of the material
K_{max}	maximum K factor during a loading cycle
K_{min}	minimum K factor during a loading cycle
L_r	ligament yielding parameter
n	fit parameter of Eq. (4)
N	number of loading cycles
N_c	critical number of loading cycles referring to component failure

POD	probability of detection of a crack in non-destructive inspection
POND	probability to miss a crack in non-destructive inspection (ND – non-detection)
R	R ratio (in damage tolerance analyses K_{\min}/K_{\max})
Q_1, Q_2, Y_1, Y_2	forces acting at the wheel (Figure 5)
r	radius of the railway axle
t	wall thickness of the hollow railway axle
T transition	geometrical transition at the axle according to Figure 5
V transition	geometrical transition at the axle according to Figure 5
ΔK	cyclic stress intensity factor ($K_{\max}-K_{\min}$)
$\Delta K_I, \Delta K_{II}, \Delta K_{III},$	cyclic stress intensity factors for mode I, II and III crack opening
ΔK_{eff}	ΔK corrected for the plasticity induced crack closure effect
ΔK_{th}	threshold of fatigue crack propagation
$\Delta K_{\text{th,eff}}$	ΔK_{th} corrected for the plasticity induced crack closure effect
ΔK_v	mixed mode equivalent cyclic stress intensity factor
μ	friction coefficient
σ	stress
σ_b	bending stress determined at the axle shaft